© 2019. Published by The Company of Biologists Ltd | Journal of Experimental Biology (2019) 222, jeb200410. doi:10.1242/jeb.200410

SHORT COMMUNICATION

Turtles maintain mitochondrial integrity but reduce mitochondrial respiratory capacity in the heart after cold acclimation and anoxia

Amanda Bundgaard[1,*], Klaus Qvortrup[2], Lene Juel Rasmussen[3] and Angela Fago[1]

ABSTRACT

Mitochondria are important to cellular homeostasis, but can become a dangerous liability when cells recover from hypoxia. Anoxia-tolerant freshwater turtles show reduced mitochondrial respiratory capacity and production of reactive oxygen species (ROS) after prolonged anoxia, but the mechanisms are unclear. Here, we investigated whether this mitochondrial suppression originates from downregulation of mitochondrial content or intrinsic activity by comparing heart mitochondria from (1) warm (25°C) normoxic, (2) cold-acclimated (4°C) normoxic and (3) cold-acclimated anoxic turtles. Transmission electron microscopy of heart ventricle revealed that these treatments did not affect mitochondrial volume density and morphology. Furthermore, neither enzyme activity, protein content nor supercomplex distribution of electron transport chain (ETC) enzymes changed significantly. Instead, our data imply that turtles inhibit mitochondrial respiration rate and ROS production by a cumulative effect of slight inhibition of ETC complexes. Together, these results show that maintaining mitochondrial integrity while inhibiting overall enzyme activities are important aspects of anoxia tolerance.

KEY WORDS: Electron microscopy, Respirometry, Mitochondria, Reactive oxygen species, Supercomplex, Oxygen

INTRODUCTION

Mitochondria are central to cellular homeostasis as the main producers of ATP, but are also essential to regulate intracellular Ca^{2+}, apoptosis, reactive oxygen species (ROS) production and cellular redox status. However, under low levels (hypoxia) or complete absence (anoxia) of oxygen, mitochondria can become a dangerous liability. Without oxygen, electron flow through the electron transport chain (ETC) is inhibited, protons can no longer be pumped across the inner mitochondrial membrane and ATP synthase (complex V) activity can be reversed to act as an ATPase in an attempt to maintain mitochondrial membrane potential (Nicholls, 1974; Scott and Nicholls, 1980). Low ATP levels can then induce opening of K_{ATP} channels, leading to depolarisation of the inner mitochondrial membrane potential, release of mitochondrial Ca^{2+} and opening of the mitochondrial transition pore to release cytochrome *c* and induce apoptosis, leading to cell death (Galli and Richards, 2014; Pamenter et al., 2008). In mammals, reoxygenation after a period of oxygen deprivation, as in ischemia and reperfusion, can lead to extensive mitochondrial production of ROS by complex I through reverse electron transfer, driven by the accumulation of the citric acid cycle metabolite succinate, thereby further contributing to tissue damage (Chouchani et al., 2014; Yellon and Hausenloy, 2007). Mammals reduce mitochondrial content by mitophagy (Zhang et al., 2008) and inhibit mitochondrial respiration rate during hypoxia (Jain et al., 2016; Kim et al., 2006; Papandreou et al., 2006; Semenza, 2013) to limit these potentially damaging effects of mitochondria (Semenza, 2007, 2013).

However, some animals such as the freshwater turtle *Trachemys scripta elegans* are very resilient to hypoxia and are able to survive several weeks in the absence of oxygen at low temperature (Ultsch, 1985, 2006; Warren et al., 2006) without suffering from significant oxidative stress at reoxygenation (Hermes-Lima and Zenteno-Savín, 2002; Willmore and Storey, 1997a). Although most tissues shut down function during anoxia (Bickler and Buck, 2007; Boutilier and St-Pierre, 2000; Guppy and Withers, 1999; Hochachka et al., 1996), the heart keeps beating, albeit at a lower rate, to circulate nutrients and waste products (Stecyk et al., 2009), and still survives prolonged anoxia without evident damage (Bundgaard et al., 2018; Wasser et al., 1992). Low temperature and suppression of energy demand enable turtles to manage to rely exclusively on glycolysis as the only source of ATP, fuelled by liver glycogen stores (Bickler and Buck, 2007; Brooks and Storey, 1989; Kelly and Storey, 1988; Warren et al., 2006). Whether mitochondrial activity is also downregulated as part of the remarkable anoxia tolerance of turtles is less well understood (Galli and Richards, 2014). It is known that mitochondria isolated from anoxic turtles have lower respiration rates (Bundgaard et al., 2018; Galli et al., 2013; Pamenter et al., 2016) and lower intrinsic capacity for ROS production (Bundgaard et al., 2018). Cold acclimation in itself leads to metabolic depression, which may prime physiological processes for prolonged anoxia (Couturier et al., 2019; Ultsch, 1985). Interestingly, cold acclimation decreases mitochondrial respiration rate in anoxia-tolerant frogs (*Rana temporaria*) (St-Pierre and Boutilier, 2001) and increases it in anoxia-intolerant brown trout (*Salmo trutta*) (Guderley et al., 1997; Kraffe et al., 2007; St-Pierre et al., 1998), but the effect of cold acclimation on mitochondrial respiration rate in turtles has not previously been investigated. Whether mitochondrial respiration rate is inhibited with cold acclimation and long-term anoxia and whether this is due to inhibition of mitochondrial complex function or to reduction in mitochondrial volume density is the focus of the present study. We have previously shown that turtle ETC complexes associate into very stable supercomplexes (Bundgaard et al., 2018), which are supposedly involved in enhancing electron transfer, thereby increasing respiration rate and reducing ROS production (Acin-Perez and Enriquez, 2014; Lapuente-Brun et al., 2013). Whether the assembly into supercomplexes is associated with reduction in mitochondrial respiration is also a question we address in this study.

[1]Department of Bioscience, Aarhus University, 8000 Aarhus, Denmark. [2]Department of Biomedical Sciences/CFIM, University of Copenhagen, 2200 Copenhagen, Denmark. [3]Center for Healthy Aging, Department of Cellular and Molecular medicine, University of Copenhagen, 2200 Copenhagen, Denmark.

*Author for correspondence (ammagabu@yahoo.dk)

A.B., 0000-0001-9716-8333; L.J.R., 0000-0001-6864-963X; A.F., 0000-0001-7315-2628

Received 25 January 2019; Accepted 11 May 2019

Journal of Experimental Biology (2019) 222, jeb200410. doi:10.1242/jeb.200410

List of symbols and abbreviations

BSA	bovine serum albumin
DDM	dodecyl maltoside
dQ	decylubiquinone
ETC	electron transport chain
HAAR	hexaaminеruthenium(III) chloride
ROS	reactive oxygen species
TEM	transmission electron microscopy
ε	molar extinction coefficient

Here, we investigate whether heart mitochondria from the anoxia-tolerant freshwater turtle are regulated during cold acclimation and long-term anoxia. Specifically, we use a combination of techniques, including high-resolution respirometry, spectrophotometric assays and transmission electron microscopy (TEM), to assess mitochondrial respiration rate, ROS production, mitochondrial content, morphology, cristae surface area, and content and activity of ETC complexes. We found that turtles maintain mitochondrial content and integrity in the heart, but inhibit mitochondrial substrate oxidation during cold acclimation and long-term anoxia.

MATERIALS AND METHODS

Chemicals

All chemicals were obtained from Sigma-Aldrich. Amplex UltraRed was obtained from Thermo Fisher Scientific.

Animals

Adult red-eared sliders, *Trachemys scripta elegans* (Wied-Neuwied 1839), of both sexes were obtained from Nasco (Fort Atkinson, WI, USA) and allowed to acclimate to captivity for several months before experimentation. Turtles were kept in aquaria at 25°C and had free access to dry platforms under infrared lamps for behavioural thermoregulation. Twelve turtles were randomly divided into three groups: a group of warm, fed turtles kept at 25°C with full access to air and basking platforms (mean±s.e.m. mass=0.63±0.05 kg, n=3) and two groups of turtles acclimated to 5°C, of which one group was exposed to 9 days of anoxia, as described in detail elsewhere (Bundgaard et al., 2018; Jensen et al., 2014). Briefly, turtles were fasted and gradually cooled to 5°C over 6 weeks before transferring one anoxic and one normoxic turtle to new aquaria per day. Anoxic turtles (0.64±0.07 kg, n=4) were kept submerged in mouse cages with a metal lid to avoid surfacing and the water was continuously bubbled with nitrogen. Normoxic turtles (0.66±0.13 kg, n=5) were kept in 10 cm of water in individual tanks. Experiments were carried out in October–November 2017 in accordance with Danish laws on animal care and experimentation under the permit 2015-15-0201-00544.

Anaesthesia and tissue sampling

Turtles were removed from the water and euthanised at room temperature by injection of 50 mg kg^{-1} pentobarbital into the supravertebral venous sinus, as described in a previous study (Bundgaard et al., 2018). When the turtles no longer responded to pinching of the legs and had no corneal reflex, they were decapitated and the brain was injected intrathecally with a lethal dose of pentobarbital. The plastron was opened with a bonesaw, the heart was dissected out and the ventricle was removed and transferred to a glass Petri dish. The dark red color of blood and heart tissue in anoxic turtles compared with normoxic ones indicated absence of reoxygenation during euthanasia. The ventricle was then washed in phosphate buffered saline (PBS) to remove blood and divided into four portions used for: (1) TEM, (2) high-resolution respirometry in permeabilised fibres and (3) high-resolution respirometry in isolated mitochondria (where ROS production was also measured). We chose to work with both permeabilised fibres and isolated mitochondria, as permeabilised fibres are assumed to be the most physiologically relevant to measure mitochondrial respiration rate, but ROS production cannot be reliably measured in permeabilised fibres owing to the oxygen gradient that can affect ROS production measurements (Kuznetsov et al., 2008). Finally, (4) a fourth portion was snap-frozen in liquid N_2 for subsequent enzyme activity assays and western blotting.

Transmission electron microscopy

The tip of the ventricle was used for TEM. The tissue was kept wet in PBS on parafilm on a glass Petri dish on ice and samples approximately 1 mm^3 were isolated using two crossed scalpel blades. The samples were subsequently fixed by immersion in 2% glutaraldehyde in 50 mmol l^{-1} $NaPO_4$, pH 7.4, at 4°C. The fixative was changed after 24 h before overnight shipping on ice to the Core Facility for Integrated Microscopy, University of Copenhagen.

Samples were rinsed three times in 150 mmol l^{-1} sodium phosphate buffer (pH 7.2) and subsequently postfixed in 1% w/v OsO_4 with 50 mmol l^{-1} $K_3Fe(CN)_6$ in 120 mmol l^{-1} sodium phosphate buffer (pH 7.2) for 2 h. The specimens were dehydrated in graded series of ethanol, transferred to propylene oxide and embedded in Epon according to standard procedures (Larsen et al., 2012). Sections approximately 60 nm thick were cut with an Ultracut 7 (Leica, Wienna, Austria) and collected on one-hole copper grids with Formvar supporting membranes, stained with uranyl acetate and lead citrate, and subsequently examined with a Philips CM 100 Transmission EM (Philips, Eindhoven, The Netherlands), operated at an accelerating voltage of 80 kV. Digital images were recorded with an OSIS Veleta digital slow scan 2k×2k CCD camera and the ITEM software package (Olympus Soft Imaging Solutions GMBH, Münster, Germany).

TEM mitochondrial analysis

Twenty to 30 micrographs of 10,400–25,000× magnification were obtained from one section per animal for quantification of mitochondrial volume density and 15 micrographs of 64,000× magnification for quantification of mitochondrial inner membrane surface density. Images were analysed with Adobe Photoshop 6.0 and overlaid with a 12×12 square lattice with spacing equal to 1 µm or 55 nm on the micrographs for mitochondrial volume density and surface density, respectively. Mitochondrial volume density was estimated by point-counting (Fig. 1) (Broskey et al., 2013; Weibel, 1979), where the relative amounts of intercepts on the grid that intercept with mitochondria in 2D reflects the relative volume of mitochondria in the 3D heart fibre, as described in detail by Weibel (1979). Mitochondrial inner membrane surface density ($S_{cr+i,mi}$) was estimated by the line-intercept method (Weibel, 1979) and calculated by:

$$S_{cr+i,mi} = (I_{cr+i}/P_{Mi}) \times (M/d_b), \quad (1)$$

where I_{cr+i} is the number of intersections of the cristae+inner mitochondrial membrane with both horizontal and vertical grid lines included within the mitochondrion in the image; P_{Mi} is the number of points in the grid within the mitochondrion where the inner membranes are not included; M is the final magnification; and d_b is the distance between lines on the grid. Extracellular matrix and luminal spaces were excluded from quantification.

Journal of Experimental Biology (2019) 222, jeb200410. doi:10.1242/jeb.200410

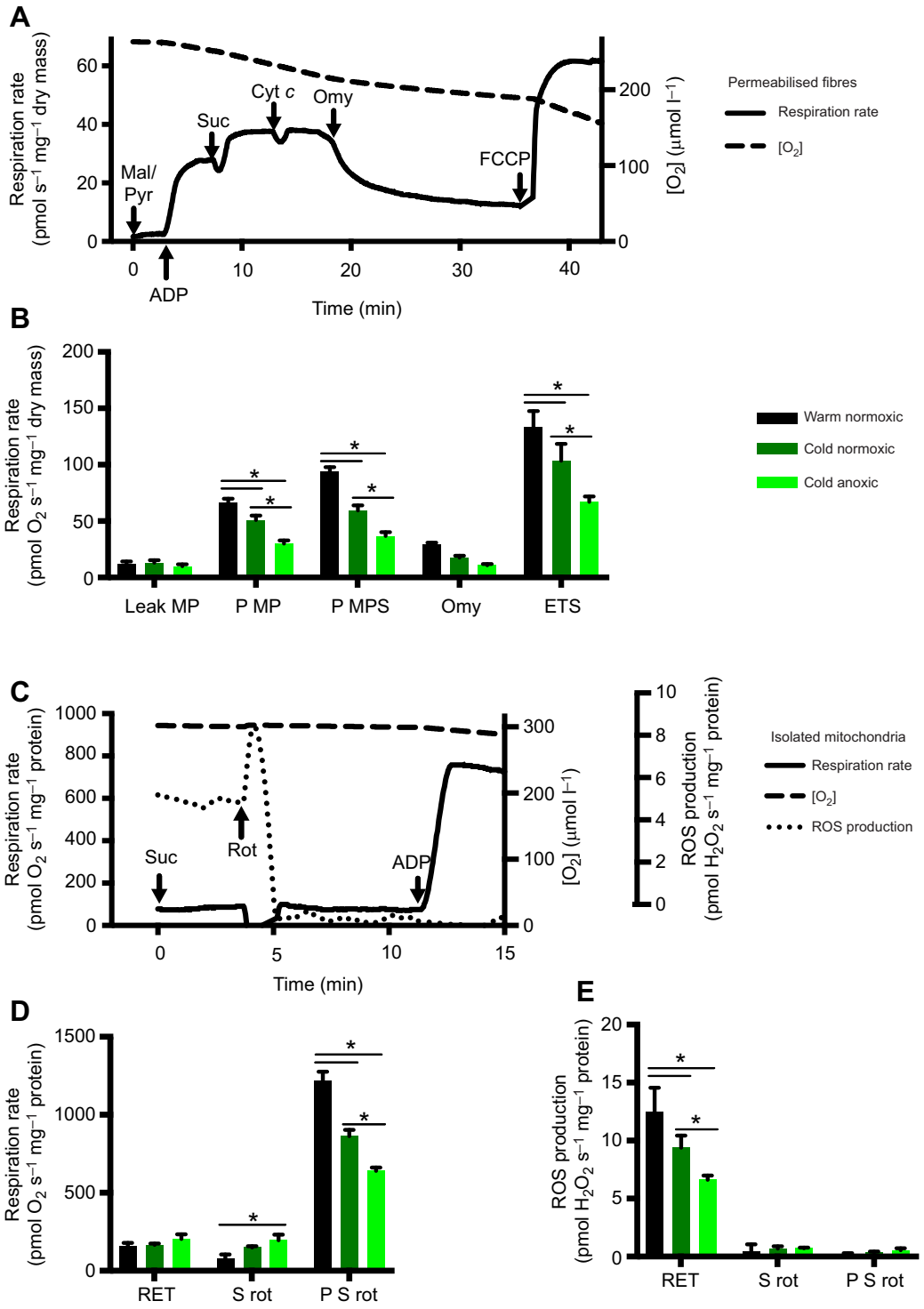

Fig. 1. Respiration rate of permeabilised fibres and isolated mitochondria from the heart of anoxic and normoxic turtles (*Trachemys scripta elegans*). (A) Representative respiration trace showing the experimental protocol (see Materials and Methods for details) and (B) respiration rates of permeabilised heart fibres. (C) Representative respiration and reactive oxygen species (ROS) trace and (D) respiration rates and (E) ROS production of isolated heart mitochondria. Mal/M, malate; Pyr/P, pyruvate; Suc/S, succinate; Cyt *c*, cytochrome *c*; Omy, oligomycin; ETS, maximal respiratory capacity; RET, reverse electron transfer; Rot: rotenone. *P<0.05 tested by one-way ANOVA. Data are shown as means±s.e.m., n=3 for warm normoxic turtles, n=5 for cold normoxic and n=4 for cold anoxic turtles.

Permeabilised fibres

A portion of the ventricle tissue was rinsed in turtle skinning solution (2 mmol l^{-1} $CaCl_2$, 10 mmol l^{-1} EGTA, 5.8 mmol l^{-1} sodium ATP, 1.4 mmol l^{-1} $MgCl_2$, 20 mmol l^{-1} Imidazole, 20 mmol l^{-1} taurine, 50 mmol l^{-1} K-MES, 15 mmol l^{-1} sodium phosphocreatine, 0.5 mmol l^{-1} DTT, pH 7.2) (Birkedal and Gesser, 2004). Fibres were gently separated with tweezers and transferred to a 2 ml Eppendorf tube with skinning solution and 50 µg ml^{-1} saponin, and gently shaken at 4°C for 30 min. The fibres were subsequently washed in respiration medium (70 mmol l^{-1} sucrose, 220 mannitol,

2 mmol l^{-1} EGTA, 5 mmol l^{-1} $MgCl_2$, 5 mmol l^{-1} KPO_4^-, 10 mmol l^{-1} Hepes, pH 7.4) for 3×10 min at 4°C on a shaker.

Isolated mitochondria

During the incubation steps in the preparation of permeabilised fibres, mitochondria were isolated from another portion of the heart ventricle as described in detail elsewhere (Bundgaard et al., 2018). Briefly, connective tissue was removed and the heart was homogenised in STE buffer (250 mmol l^{-1} sucrose, 5 mmol l^{-1} Tris, 1 mmol l^{-1} EGTA, pH 7.4) with 0.5% bovine serum albumin (BSA) on ice. The homogenate was centrifuged at 700 ***g*** for 5 min at 4°C, and the supernatant was filtered through cheesecloth and centrifuged at 10,000 ***g*** for 10 min at 4°C twice, washing away the fluffy layer with damaged mitochondria, before finally resuspending the mitochondrial pellet in a minimal amount of STE without BSA. Protein content was determined with the Pierce 660 nm protein assay with BSA as standard.

Respiration rate and ROS production

Respiration rate and ROS production were measured simultaneously with an Oroboros Oxygraph 2K high-resolution respirometry system fitted with an O2K-fluorescence LED2 module with filters specific for the Amplex UltraRed product resorufin (Oroboros Instruments, Innsbruck, Austria). The O_2 electrodes were calibrated daily with air-saturated respiration medium, and all measurements were conducted at 13°C. Two different protocols were employed, one for permeabilised fibres measuring respiration rate and one for isolated mitochondria measuring respiration rate and ROS production with Amplex UltraRed. All respiration rate measurements were corrected for non-mitochondrial oxygen consumption by subtracting the background respiration rate obtained with the complex III inhibitor antimycin A.

Permeabilised fibres (~1 mg dry mass) were added to the chambers and the respiration protocol was run in duplicate; the complex I-dependent substrates malate (2.5 mmol l^{-1}) and pyruvate (5 mmol l^{-1}) were added to initiate state II (non-phosphorylating) respiration, before ADP (1 mmol l^{-1}) was added to start complex I-dependent state III (phosphorylating) respiration. Succinate (10 mmol l^{-1}) was then added to measure complex I+II state III respiration rate, and cytochrome *c* (10 µmol l^{-1}) was added to test the integrity of the outer mitochondrial membrane, which did not increase respiration rate with more than 5% in any experiments. The complex V inhibitor oligomycin was then added, and finally the mitochondria were fully uncoupled by titrating carbonyl cyanide *p*-trifluoro-methoxyphenyl hydrazine to measure maximum respiratory capacity of the ETC. The fibres were subsequently dried at 70°C for 1 h to determine dry mass of the fibres.

Isolated mitochondria (~62 µg protein ml^{-1}) were added to the chamber with 10 µmol l^{-1} Amplex UltraRed, 1 U ml^{-1} superoxide dismutase and 5 U ml^{-1} horseradish peroxidase, and the fluorometric sensors were calibrated with injections of 0.1 µmol l^{-1} H_2O_2. Maximal ROS production was measured as reverse electron transfer in the presence of 10 mmol l^{-1} succinate, and the complex I dependent part of this was estimated by addition of 8 µmol l^{-1} rotenone, before 1 mmol l^{-1} ADP was added to measure complex II-dependent state III respiration rate.

Enzyme activity assays

Sample preparation

Turtle heart ventricle samples were homogenised in four volumes (w/w) (total dilution 1:5) of 25 mmol l^{-1} potassium phosphate buffer, pH 7.2, in Precellys hard tissue homogenising tubes for 2×15 s at a speed of 6500 rpm on a Precellys 24 tissue homogeniser (Bertin Instruments, Montigny-le-Bretonneux, France) and cooled on ice between homogenising sessions. The homogenate was subsequently centrifuged for 10 min at 17,000 ***g*** at 4°C, and the pellet was resuspended, aliquoted and stored at −80°C until assaying. Enzyme activity was assayed on the first thaw. All enzyme activity assays were measured at 25°C on a SpectraMax 384 plus microplate reader (Molecular Devices, San Jose, CA, USA) in the presence of 0.05% dodecyl maltoside (DDM) to permeabilise intact mitochondria and allow access of substrates to the matrix side of the membrane proteins.

Complex I – decylubiquinone (dQ)

Activity was assayed based on Trounce et al. (1996) as the rotenone-sensitive disappearance of NADH at 340–380 nm using ε_{NADH} (340–380 nm, where ε is the molar extinction coefficient)= 6.22 l $mmol^{-1}$ cm^{-1} (Estornell et al., 1993) in 120 mmol l^{-1} KCl, 1 mmol l^{-1} EDTA, 10 mmol l^{-1} Hepes, pH 7.2, with 200 µmol l^{-1} dQ as the electron acceptor, 2 mmol l^{-1} KCN to inhibit complex IV, 300 nmol l^{-1} antimycin A to inhibit complex III, 0.05% DDM and 0.8 mmol l^{-1} NADH, with and without 10 µmol l^{-1} rotenone. This assay measures the coupled oxidation of NADH at the flavin site of complex I to reduction of ubiquinone in the membrane part of the complex.

Complex I – HAAR

Activity of the complex I flavin group was assayed as the disappearance of NADH at 340–380 nm using ε_{NADH} (340–380 nm)=6.22 l $mmol^{-1}$ cm^{-1} (Estornell et al., 1993) in 120 mmol l^{-1} KCl, 1 mmol l^{-1} EDTA, 10 mmol l^{-1} Hepes, pH 7.2, with 2 mmol l^{-1} hexaammineruthenium(III) chloride (HAAR) as the electron acceptor, 2 mmol l^{-1} KCN, 300 nmol l^{-1} antimycin A, 0.05% DDM and 0.8 mmol l^{-1} NADH. This assay measures activity of the flavin site at the matrix arm of complex I, which is independent of the membrane part of the enzyme.

Complex II

Activity was assayed based on Hatefi and Stiggall (1978) as the disappearance of 2,6-dichlorophenolindophenol (DCPIP) at 600 nm using ε_{DCPIP} (600 nm)=19.1 l $mmol^{-1}$ cm^{-1} (Spinazzi et al., 2012), with and without 200 µmol l^{-1} of the complex II inhibitor 2-theonyltrifluoroacetone (TTFA) in 50 mmol l^{-1} potassium phosphate buffer, 0.1 mmol l^{-1} EDTA, 0.01% Triton-X-100, pH 7.4, with 20 mmol l^{-1} succinate, 75 µmol l^{-1} DCPIP, 80 µmol l^{-1} decylubiquinone, 2 mmol l^{-1} KCN, 10 µmol l^{-1} rotenone and 300 nmol l^{-1} antimycin A.

Complex III

Complex III activity was assayed based on Hatefi (1978) as the myxothiazol-sensitive increase in reduced cytochrome *c* oxidase at 550 nm using $\varepsilon_{red\ cyt\ c}$ (550 nm)=21 l $mmol^{-1}$ cm^{-1} (Hatefi, 1978). Homogenate was added to buffer (25 mmol l^{-1} potassium phosphate buffer, pH 7.4) with 0.2 mmol l^{-1} KCN, 8 µg ml^{-1} rotenone and 100 µmol l^{-1} bovine cytochrome *c*, with and without 4 µmol l^{-1} myxothiazol. The assay was initiated by addition of 0.1 mmol l^{-1} decylubiquinol.

Complex IV

Activity was assayed based on Errede et al. (1978) as the cyanide-sensitive oxidation of cytochrome *c* at 550 nm using $\varepsilon_{red\ cyt\ c}$ (550 nm)=21 l $mmol^{-1}$ cm^{-1} (Hatefi, 1978) in buffer (200 mmol l^{-1} Tris, 10 µmol l^{-1} EDTA, pH 7.5) with 0.3%

Tween-80, 300 nmol l^{-1} antimycin A, 10 µmol l^{-1} rotenone and 100 µmol l^{-1} reduced cytochrome *c*, with and without 2 mmol l^{-1} KCN. Reduced cytochrome *c* was prepared by addition of sodium dithionite to a 6 mmol l^{-1} stock of cytochrome *c* in 200 mmol l^{-1} Tris, pH 7.5, followed by gel-filtration through a Sephadex G-25 column to remove dithionite.

Complex V

Complex V activity was assayed as previously described (Pullman et al., 1960) as the oligomycin-sensitive decrease in NADH using ε_{NADH} (340–380 nm)=6.22 l $mmol^{-1}$ cm^{-1} (Estornell et al., 1993). Homogenate was added to 100 mmol l^{-1} Tris buffer, 50 mmol l^{-1} KCl, 2 mmol l^{-1} $MgCl_2$, 0.2 mmol l^{-1} EDTA, pH 8.0, with 1 mmol l^{-1} phosphoenolpyruvate, 2.5 mmol l^{-1} ATP, 2 U ml^{-1} lactate dehydrogenase and 4 U ml^{-1} pyruvate kinase, and the assay was initiated by addition of 0.8 mmol l^{-1} NADH. Rotenone (10 µmol l^{-1}), antimycin A (300 nmol l^{-1}) and KCN (2 mmol l^{-1}) were added to exclude background NADH oxidation, and oligomycin (2 µmol l^{-1}) was added to correct for non-specific activity.

Citrate synthase

Mitochondrial content was estimated by activity of the matrix enzymes citrate synthase and glutamate dehydrogenase. Citrate synthase activity was measured as the formation of 2-nitro-5-thiobenzoic acid (TNB) at 412 nm using ε_{TNB} (412 nm)=13,600 l $mmol^{-1}$ cm^{-1} as described in Srere (1969). Homogenate was added to 100 mmol l^{-1} Tris, pH 8.0, with 0.1% (v/v) Triton-X-100, 370 µmol l^{-1} acetyl CoA and 100 µmol l^{-1} 5,5′-dithiobis(2-nitrobenzoic acid) (DTNB), and the assay was initiated by addition of 66 µmol l^{-1} oxaloacetate.

Glutamate dehydrogenase

Glutamate dehydrogenase activity was assayed as the disappearance of NADH using ε_{NADH} (340–380 nm)=6.22 l $mmol^{-1}$ cm^{-1} (Estornell et al., 1993). Homogenate was added to 85 mmol l^{-1} imidazole, 1 mmol l^{-1} EDTA, 220 mmol l^{-1} ammonium acetate, pH 7.4, with 0.1% Triton-X-100, 10 mmol l^{-1} 2-oxoglutarate and 1 mmol l^{-1} ADP, before 0.8 mmol l^{-1} NADH was added to initiate the reaction.

Western blotting

Heart homogenate for western blotting was prepared as described for enzyme activity assays, but in 100 mmol l^{-1} Tris buffer, pH 7.5, with protease inhibitor tablets (cOmplete Mini, EDTA-free, Sigma-Aldrich). Proteins were denatured in SDS-PAGE loading buffer with 50 mmol l^{-1} DTT for 5 min at 95°C before loading 30 µg protein per lane on a 10% 15-well BioRad Protean TGX gel and run at 120 V for 80 min. Proteins were then transferred to a PVDF membrane (BioRad) on a Trans-Blot semi-dry transfer cell (BioRad) at 25 V for 7 min. The membrane was blocked in Odyssey blocking buffer (LI-COR Biotechnology, Lincoln, NE, USA) for 1 h and incubated overnight with primary antibodies: 1:1000 anti-NDUFS3 (complex I, Abcam), 1:5000 anti-SDHA (complex II, Abcam), 1:1000 anti-ATP5A (complex V, Abcam), 1:1500 GAPDH (Abcam) and 1:500 TOM20 (Santa Cruz Biotechnology). TOM20 is a mitochondrial membrane protein that can be used as a measure of mitochondrial content (Latorre-Pellicer et al., 2016). The next day, the membrane was washed in PBS+0.02% TWEEN-20 and incubated with 1:20,000 secondary goat anti-mouse antibody (IRDye, 800 CW, LI-COR Biotechnology) and developed for near-infrared fluorescence on an Odyssey CLx imaging system (LI-COR Biotechnology). Protein content was quantified with the ImageJ Gel Analysis software (version 1.51m9, National Institutes of Health, Bethesda, MD, USA), and was standardised to the loading control GAPDH.

Blue native-PAGE

Mitochondrial membrane proteins were extracted with 1.25% DDM and separated by BN-PAGE as described in detail elsewhere (Bundgaard et al., 2018). Complex I activity was identified in gels as a purple activity staining by incubation with 150 µmol l^{-1} NADH and 1 mg ml^{-1} nitroblue tetrazolium for 20 min (Van Coster et al., 2001).

Statistics

Data were analysed using one-way ANOVA with Tukey's multiple comparisons test for normally distributed data (Prism 7, GraphPad Software, San Diego, CA, USA), and statistical significance was assumed when $P<0.05$. All data are shown as means±s.e.m.

RESULTS AND DISCUSSION

In this study, we investigated whether anoxia-tolerant freshwater turtles downregulate mitochondrial content or function of key enzymes during cold acclimation and prolonged anoxia as part of their remarkable anoxia tolerance. Our results show that both respiration rate (Fig. 1A–D) and ROS production (Fig. 1C,E) decreased with fasting and cold acclimation and decreased further with exposure of cold-acclimated turtles to anoxia. Phosphorylating state III respiration rate, which reflects both the substrate oxidation rate that produces the proton motive force across the inner mitochondrial membrane and the rate of ATP turnover that consumes it, decreased by ∼30% with cold acclimation and further by ∼40% with anoxia in both permeabilised heart fibres (Fig. 1A,B) and isolated mitochondria (Fig. 1C,D). This suggests that the decrease is due to inhibition of the intrinsic activity of mitochondrial complexes rather than to the mitochondrial content of the cardiomyocytes. The fully uncoupled respiration rate, which represents substrate oxidation by the ETC independent of ATP synthase, decreased by ∼25% and ∼35% with cold acclimation and anoxia, respectively (Fig. 1A,B). Thus, up to 80% of the observed reduction in respiration rate with cold acclimation and anoxia was due to a reduction in substrate oxidation, with the remaining part due to a reduction in the ATP turnover. This is consistent with a previous study on hepatopancreas mitochondria from snails exposed to hypoxia, where 75% of the inhibition of mitochondrial respiration with hypoxia was attributed to inhibition of substrate oxidation (Bishop et al., 2002). Leak respiration, which reflects the proton conductance of the inner mitochondrial membrane, did not change with cold acclimation or anoxia (Fig. 1B), as also found in a previous study on anoxic turtle heart mitochondria (Galli et al., 2013), reflecting membrane lipid composition. Therefore, mitochondrial respiration rate in anoxic turtles is not modulated by changes in the proton conductance of the inner membrane.

These results show that mitochondrial respiration rate is inhibited with both cold acclimation and anoxia in the turtle heart. Cold acclimation also leads to inhibition of mitochondrial respiration rate in another anoxia-tolerant vertebrate, the common frog (*Rana temporaria*) (St-Pierre and Boutilier, 2001), but not in brown trout (Guderley et al., 1997; Kraffe et al., 2007; St-Pierre et al., 1998). This suggests that inhibition of mitochondrial respiration rate contributes to metabolic depression with cold acclimation, and that this may be a key part of anoxia tolerance. Our results are also consistent with studies on isolated mitochondria from anoxic turtles (Bundgaard et al., 2018; Galli et al., 2013; Pamenter et al., 2016) as well as others on anoxia-tolerant animals exposed to hypoxia, such as frogs

Journal of Experimental Biology (2019) 222, jeb200410. doi:10.1242/jeb.200410

(St-Pierre et al., 2000b), killifish (*Fundulus heteroclitus*) (Du et al., 2016; Duerr and Podrabsky, 2010), epaulette sharks (*Hemiscyllum ocellatum*) and shovel-nosed rays (*Aptychotrema rostrata*) (Hickey et al., 2012). Inhibition of mitochondrial respiration rate is also central to the response to hypoxia in mammalian cells (Kim et al., 2006; Papandreou et al., 2006; Semenza, 2007). Thus, the inhibition of mitochondrial respiration rate is a general response to hypoxia.

To establish that mitochondrial content was unchanged with cold acclimation and anoxia and to assess the mitochondrial morphology, we then performed a detailed ultrastructural study of cardiac fibres from the three experimental groups. These experiments revealed no qualitative alterations in mitochondrial shape or distribution within the heart ventricle and no quantitative changes in volume density or mitochondrial inner membrane surface area (Fig. 2A–E). Lipid droplets were significantly more abundant in samples from anoxic turtle hearts (Fig. 2F,G), reflecting a metabolic shift away from fatty acid oxidation in the absence of oxygen, consistent with previous studies on turtle hearts (Almeida-Val et al., 1994; Bundgaard et al., 2019). Furthermore, there was no significant change in the activity of the mitochondrial marker enzymes citrate synthase (Fig. 3F) and glutamate dehydrogenase (Fig. 3G), nor in the expression of the mitochondrial membrane marker protein TOM20 (Fig. 3I). Together, these results show that turtle hearts maintain mitochondrial content and integrity even when metabolic rate is low and when oxygen is absent. This contrasts with the hypoxic response in anoxia-susceptible mammals, where mitochondrial content decreases owing to mitophagy, possibly in order to limit oxidative damage from mitochondrial ROS (Zhang et al., 2008). Instead, anoxia-tolerant turtles limit oxidative damage at reoxygenation in the heart by inhibiting the maximal capacity for mitochondrial ROS

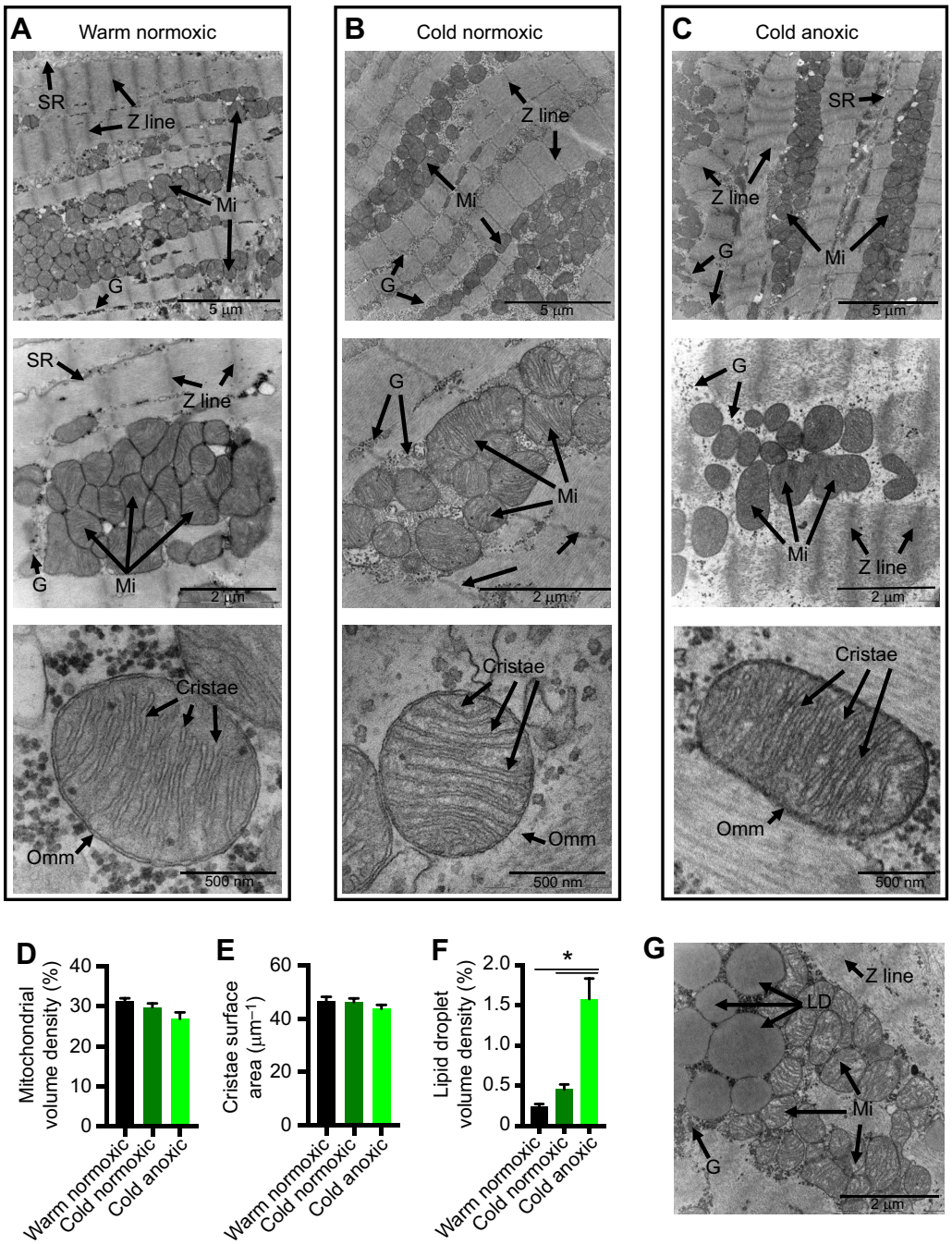

Fig. 2. Transmission electron microscopy and analysis of mitochondrial morphology in turtle hearts. Micrographs of (A) warm normoxic, (B) cold normoxic and (C) cold anoxic turtle hearts. Quantification of (D) mitochondrial volume density and (E) surface volume showed no significant differences between groups. (F) Volume density of fatty acid droplets and (G) high magnification of lipid droplets in an anoxic turtle heart sample image. G, glycogen grains; LD, lipid droplet; Mi, mitochondria; Omm, outer mitochondrial membrane; SR, sarcoplasmic reticulum. Statistical details described in Fig. 1.

Journal of Experimental Biology (2019) 222, jeb200410. doi:10.1242/jeb.200410

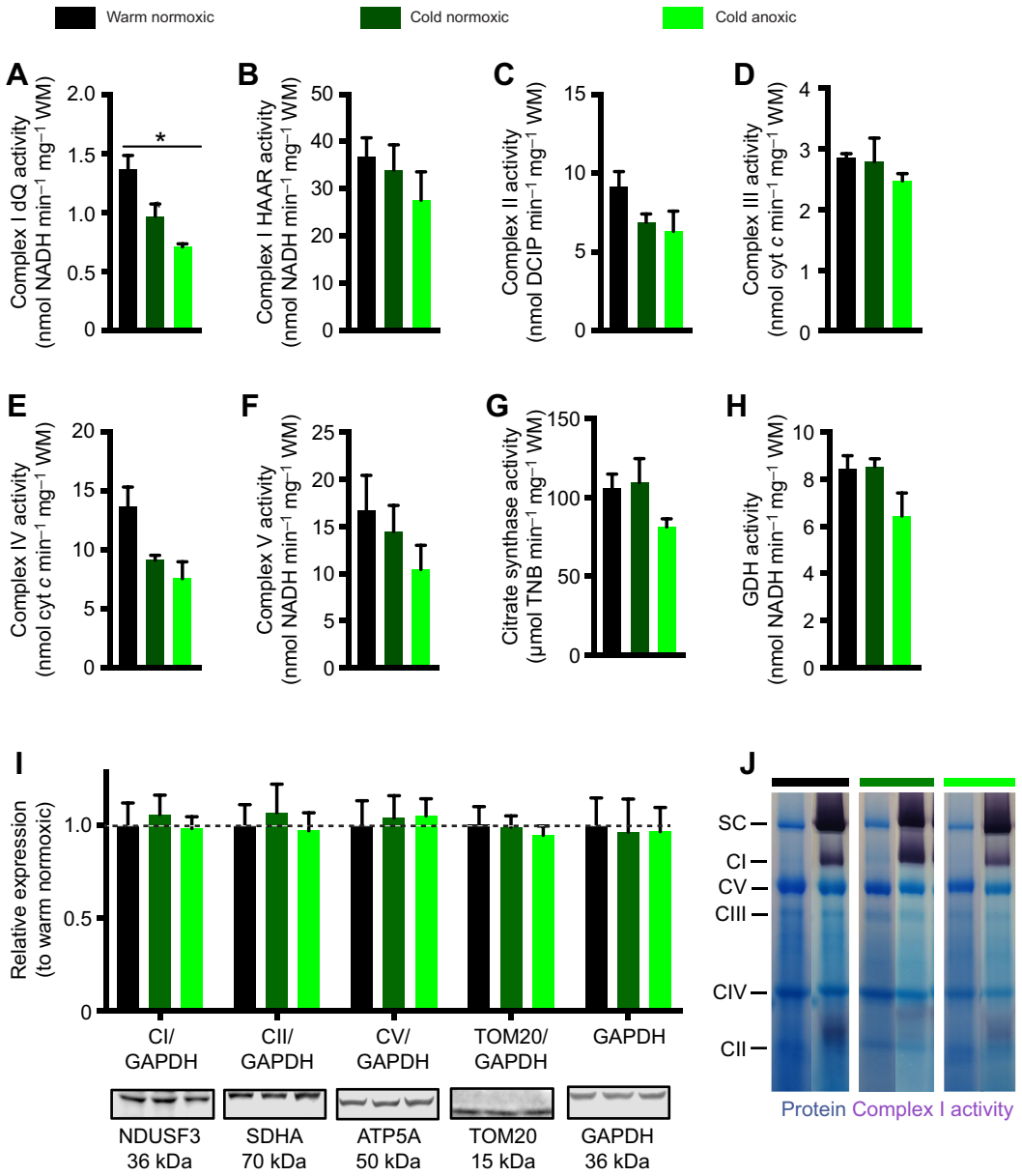

Fig. 3. Activity of mitochondrial enzymes and analysis of supercomplex (SC) assembly in turtle heart homogenates. Enzyme activity of turtle heart homogenate of complex I NADH dehydrogenase with (A) dQ and (B) HAAR as electron acceptor, (C) complex II succinate dehydrogenase with DCIP as electron acceptor, (D) complex III cytochrome *c* reductase, (E) complex IV cytochrome *c* oxidase, (F) complex V ATPase, (G) citrate synthase DTNB reduction and (H) glutamate dehydrogenase (GDH). (I) Western blot of turtle heart mitochondrial proteins and (J) distribution of mitochondrial complexes by BN-PAGE with 1.25% DDM. Blue stain indicate protein bands, purple stain indicates complex I activity. WM, wet mass. Statistical details are described in Fig. 1.

production via reverse electron transfer (Fig. 1C,E), in addition to limiting the accumulation of succinate and maintaining sufficient ADP to prevent reverse electron transfer at reoxygenation (Bundgaard et al., 2019). Antioxidant capacity of the turtle heart has been reported to decrease during anoxia (Willmore and Storey, 1997a,b), which would be inefficient in terms of ROS scavenging at reoxygenation.

Mitochondrial morphology, such as cristae structure and the surface area of the inner mitochondrial membrane, affects the activity of the ETC (Schwerzmann et al., 1989). However, neither mitochondrial morphology, cristae structure (Fig. 2A–C) nor surface area of the inner mitochondrial membrane (Fig. 2E) differed between experimental groups, indicating that the turtle heart maintains mitochondrial content and morphology during metabolic depression and anoxia and that cristae remodelling is not part of the inhibition of mitochondrial respiration rate.

Instead, up to 80% of mitochondrial respiration rate is decreased by inhibition of mitochondrial substrate oxidation. This inhibition must be conveyed by modulation of the enzymes of the citric acid cycle or ETC involved in substrate oxidation. Maximal enzyme activity of the ETC complexes (complexes I–V) (Fig. 3A–H) and expression of complexes I, II and V (Fig. 3I) were not significantly different between experimental groups, except complex I dQ activity, which was significantly lower between the warm normoxic and anoxic groups (Fig. 3A). However, there was a general trend towards lower ETC enzyme activity with metabolic depression (Fig. 3A–H). This suggests that the reduced mitochondrial respiration rate with cold acclimation (Fig. 1) may be caused by a cumulative effect of slight inhibitions of ETC enzymes, rather than by a strong inhibition on one or few such enzymes. Considering that the ETC enzymes work in series, a slight and statistically

insignificant decrease in the activity of individual complexes would result in an overall significant inhibition at the level of the entire ETC. The modulation of enzyme activity could originate from post-translational modifications (Krivoruchko and Storey, 2015) or subunit substitution of individual complexes (Fukuda et al., 2007). In contrast to previous studies on turtles (Galli et al., 2013; Pamenter et al., 2016) and frogs (St-Pierre et al., 2000a), we did not find a significant decrease in complex V activity, which is likely due to methodological differences. Although complex V inhibition could in principle contribute to inhibit mitochondrial ATP turnover and thereby mitochondrial respiration rate, complex V inhibition cannot be the main source of inhibition of mitochondrial respiration rate in the anoxic turtle heart, as ATP turnover is only responsible for less than 20% of the inhibition of mitochondrial respiration rate (Fig. 1), as discussed above.

Modulation of mitochondrial supercomplexes, the structural association of complex I and complex III with or without complex IV (Letts et al., 2016), is another potential way of regulating ETC complex activity to inhibit mitochondrial substrate oxidation (Acin-Perez and Enriquez, 2014; Lapuente-Brun et al., 2013). Supercomplexes have been identified recently and proposed to increase the efficiency of electron transfer to increase respiratory efficiency and decrease ROS production (Acin-Perez and Enriquez, 2014; Genova and Lenaz, 2014; Lapuente-Brun et al., 2013; Lopez-Fabuel et al., 2016; Maranzana et al., 2013; Milenkovic et al., 2017). We have previously shown that unlike mammalian supercomplexes, turtle supercomplexes are stable in the presence of the detergent DDM, suggesting that they are also very stable *in vivo* (Bundgaard et al., 2018). However, we did not observe any differences in supercomplex composition or stability between experimental groups (Fig. 3J), so modulation of electron transfer via different assembly into supercomplexes does not seem to be a strategy to reduce mitochondrial respiration rate and ROS production with cold acclimation and anoxia in turtles.

In summary, the data presented here show that turtles maintain mitochondrial content and integrity in the heart during cold acclimation and anoxia. Specifically, they do not reduce mitochondrial content, morphology or inner mitochondrial membrane surface area. Rather, turtles reduce mitochondrial substrate oxidation to inhibit mitochondrial respiration rate. Our data suggest that this is due to a concerted downregulation of several mitochondrial complex activities, possibly involving labile post-translational modifications and changes in subunit composition but not in supercomplex assembly. Together, these data show that inhibition of intrinsic mitochondrial activity while preserving mitochondrial content and morphology is an integral part of the remarkable anoxia tolerance of freshwater turtles.

Acknowledgements
We thank Dr Clara Prats Gavalda and Dr Cristiano Di Benedetto for TEM sample preparation and Dr Tillmann Pape for technical assistance with the imaging.

Competing interests
The authors declare no competing or financial interests.

Author contributions
Conceptualization: A.B., A.F.; Methodology: A.B., K.Q.; Formal analysis: A.B.; Investigation: A.B.; Resources: K.Q., L.J.R., A.F.; Writing - original draft: A.B.; Writing - review & editing: A.B., L.J.R., A.F.; Visualization: A.B.; Supervision: A.F.; Project administration: A.F.; Funding acquisition: A.B., L.J.R., A.F.

Funding
The work was supported by the Independent Research Fund Denmark (Danmarks Frie Forskningsfond), Natural Sciences (grant 4181-00094 to A.F.), by Nordea-fonden and Olav Thon Foundation (to L.J.R.), and by travel grants from the Graduate School of Science and Technology, Aarhus University, and the Niels Bohr Foundation (Niels Bohr Fondet) (to A.B.).

References
Acin-Perez, R. and Enriquez, J. A. (2014). The function of the respiratory supercomplexes: the plasticity model. *Biochim. Biophys. Acta Bioenerg.* **1837**, 444-450. doi:10.1016/j.bbabio.2013.12.009

Almeida-Val, V. M., Buck, L. T. and Hochachka, P. W. (1994). Substrate and acute temperature effects on turtle heart and liver mitochondria. *Am. J. Physiol.* **266**, R858-R862. doi:10.1152/ajpregu.1994.266.3.R858

Bickler, P. E. and Buck, L. T. (2007). Hypoxia tolerance in reptiles, amphibians, and fishes: life with variable oxygen availability. *Annu. Rev. Physiol.* **69**, 145-170. doi:10.1146/annurev.physiol.69.031905.162529

Birkedal, R. and Gesser, H. (2004). Effects of hibernation on mitochondrial regulation and metabolic capacities in myocardium of painted turtle (*Chrysemys picta*). *Comp. Biochem. Physiol. A Mol. Integr. Physiol.* **139**, 285-291. doi:10.1016/j.cbpb.2004.09.023

Bishop, T., St-Pierre, J. and Brand, M. D. (2002). Primary causes of decreased mitochondrial oxygen consumption during metabolic depression in snail cells. *Am. J. Physiol. Regul. Integr. Comp. Physiol.* **282**, R372-R382. doi:10.1152/ajpregu.00401.2001

Boutilier, R. G. and St-Pierre, J. (2000). Surviving hypoxia without really dying. *Comp. Biochem. Physiol. A Mol. Integr. Physiol.* **126**, 481-490. doi:10.1016/S1095-6433(00)00234-8

Brooks, S. P. and Storey, K. B. (1989). Regulation of glycolytic enzymes during anoxia in the turtle *Pseudemys scripta*. *Am. J. Physiol.* **257**, R278-R283. doi:10.1152/ajpregu.1989.257.2.R278

Broskey, N. T., Daraspe, J., Humbel, B. M. and Amati, F. (2013). Skeletal muscle mitochondrial and lipid droplet content assessed with standardized grid sizes for stereology. *J. Appl. Physiol.* **115**, 765-770. doi:10.1152/japplphysiol.00063.2013

Bundgaard, A., James, A. M., Joyce, W., Murphy, M. P. and Fago, A. (2018). Suppression of reactive oxygen species generation in heart mitochondria from anoxic turtles: the role of complex I S-nitrosation. *J. Exp. Biol.* **221**, jeb174391. doi:10.1242/jeb.174391

Bundgaard, A., James, A. M., Gruszczyk, A. V., Martin, J., Murphy, M. P. and Fago, A. (2019). Metabolic adaptations during extreme anoxia in the turtle heart and their implications for ischemia-reperfusion injury. *Sci. Rep.* **9**, 2850. doi:10.1038/s41598-019-39836-5

Chouchani, E. T., Pell, V. R., Gaude, E., Aksentijević, D., Sundier, S. Y., Robb, E. L., Logan, A., Nadtochiy, S. M., Ord, E. N. J., Smith, A. C. et al. (2014). Ischaemic accumulation of succinate controls reperfusion injury through mitochondrial ROS. *Nature* **515**, 431-435. doi:10.1038/nature13909

Couturier, C. S., Stecyk, J. A. W., Ellefsen, S., Sandvik, G. K., Milton, S. L., Prentice, H. M. and Nilsson, G. E. (2019). The expression of genes involved in excitatory and inhibitory neurotransmission in turtle (*Trachemys scripta*) brain during anoxic submergence at 21°C and 5°C reveals the importance of cold as a preparatory cue for anoxia survival. *Comp. Biochem. Physiol. D Genomics Proteomics* **30**, 55-70. doi:10.1016/j.cbd.2018.12.010

Du, S. N. N., Mahalingam, S., Borowiec, B. G. and Scott, G. R. (2016). Mitochondrial physiology and reactive oxygen species production are altered by hypoxia acclimation in killifish (*Fundulus heteroclitus*). *J. Exp. Biol.* **219**, 1130-1138. doi:10.1242/jeb.132860

Duerr, J. M. and Podrabsky, J. E. (2010). Mitochondrial physiology of diapausing and developing embryos of the annual killifish *Austrofundulus limnaeus*: implications for extreme anoxia tolerance. *J. Comp. Physiol. B Biochem. Syst. Environ. Physiol.* **180**, 991-1003. doi:10.1007/s00360-010-0478-6

Errede, B., Kamen, M. D. and Hatefi, Y. (1978). Preparation and properties of complex IV (Ferrocytochrome c: oxygen oxidoreductase EC 1.9.3.1). *Methods Enzymol.* **53**, 40-47. doi:10.1016/S0076-6879(78)53011-5

Estornell, E., Fato, R., Pallotti, F. and Lenaz, G. (1993). Assay conditions for the mitochondrial NADH:coenzyme Q oxidoreductase. *FEBS Lett.* **332**, 127-131. doi:10.1016/0014-5793(93)80498-J

Fukuda, R., Zhang, H., Kim, J., Shimoda, L., Dang, C. V. and Semenza, G. L. (2007). HIF-1 regulates cytochrome oxidase subunits to optimize efficiency of respiration in hypoxic cells. *Cell* **129**, 111-122. doi:10.1016/j.cell.2007.01.047

Galli, G. L. J. and Richards, J. G. (2014). Mitochondria from anoxia-tolerant animals reveal common strategies to survive without oxygen. *J. Comp. Physiol. B Biochem. Syst. Environ. Physiol.* **184**, 285-302. doi:10.1007/s00360-014-0806-3

Galli, G. L. J., Lau, G. Y. and Richards, J. G. (2013). Beating oxygen: chronic anoxia exposure reduces mitochondrial F_1F_O-ATPase activity in turtle (*Trachemys scripta*) heart. *J. Exp. Biol.* **216**, 3283-3293. doi:10.1242/jeb.087155

Genova, M. L. and Lenaz, G. (2014). Functional role of mitochondrial respiratory supercomplexes. *Biochim. Biophys. Acta* **1837**, 427-443. doi:10.1016/j.bbabio.2013.11.002

Guderley, H., St. Pierre, J., Couture, P., Couture, P. and Hulbert, A. J. (1997). Plasticity of the properties of mitochondria from rainbow trout red muscle with seasonal acclimatization. *Fish Physiol. Biochem.* **16**, 531-541. doi:10.1023/A:1007708826437

Guppy, M. and Withers, P. (1999). Metabolic depression in animals: physiological perspectives and biochemical generalizations. *Biol. Rev. Camb. Philos. Soc.* **74**, 1-40. doi:10.1017/S0006323198005258

Hatefi, Y. (1978). Preparation and properties of dihydroubiquinone: cytochrome *c* oxidoreductase (complex III). *Methods Enzymol.* **53**, 35-40. doi:10.1016/S0076-6879(78)53010-3

Hatefi, Y. and Stiggall, D. L. (1978). Preparation and properties of succinate: ubiquinone oxidoreductase (complex II). *Methods Enzymol.* **53**, 21-27. doi:10.1016/S0076-6879(78)53008-5

Hermes-Lima, M. and Zenteno-Savín, T. (2002). Animal response to drastic changes in oxygen availability and physiological oxidative stress. *Comp. Biochem. Physiol. C Toxicol. Pharmacol.* **133**, 537-556. doi:10.1016/S1532-0456(02)00080-7

Hickey, A. J. R., Renshaw, G. M. C., Speers-Roesch, B., Richards, J. G., Wang, Y., Farrell, A. P. and Brauner, C. J. (2012). A radical approach to beating hypoxia: depressed free radical release from heart fibres of the hypoxia-tolerant epaulette shark (*Hemiscyllum ocellatum*). *J. Comp. Physiol. B Biochem. Syst. Environ. Physiol.* **182**, 91-100. doi:10.1007/s00360-011-0599-6

Hochachka, P. W., Buck, L. T., Doll, C. J. and Land, S. C. (1996). Unifying theory of hypoxia tolerance: molecular/metabolic defense and rescue mechanisms for surviving oxygen lack. *Proc. Natl. Acad. Sci. USA* **93**, 9493-9498. doi:10.1073/pnas.93.18.9493

Jain, I. H., Zazzeron, L., Goli, R., Alexa, K., Schatzman-Bone, S., Dhillon, H., Goldberger, O., Peng, J., Shalem, O., Sanjana, N. E. et al. (2016). Hypoxia as a therapy for mitochondrial disease. *Science* **352**, 54-61. doi:10.1126/science.aad9642

Jensen, F. B., Hansen, M. N., Montesanti, G. and Wang, T. (2014). Nitric oxide metabolites during anoxia and reoxygenation in the anoxia-tolerant vertebrate *Trachemys scripta*. *J. Exp. Biol.* **217**, 423-431. doi:10.1242/jeb.093179

Kelly, D. A. and Storey, K. B. (1988). Organ-specific control of glycolysis in anoxic turtles. *Am. J. Physiol. Regul. Integr. Comp. Physiol.* **255**, R774-R779. doi:10.1152/ajpregu.1988.255.5.R774

Kim, J.-W., Tchernyshyov, I., Semenza, G. L. and Dang, C. V. (2006). HIF-1-mediated expression of pyruvate dehydrogenase kinase: a metabolic switch required for cellular adaptation to hypoxia. *Cell Metab.* **3**, 177-185. doi:10.1016/j.cmet.2006.02.002

Kraffe, E., Marty, Y. and Guderley, H. (2007). Changes in mitochondrial oxidative capacities during thermal acclimation of rainbow trout *Oncorhynchus mykiss*: roles of membrane proteins, phospholipids and their fatty acid compositions. *J. Exp. Biol.* **210**, 149-165. doi:10.1242/jeb.02628

Krivoruchko, A. and Storey, K. B. (2015). Turtle anoxia tolerance: biochemistry and gene regulation. *Biochim. Biophys. Acta Gen. Subj.* **1850**, 1188-1196. doi:10.1016/j.bbagen.2015.02.001

Kuznetsov, A. V., Veksler, V., Gellerich, F. N., Saks, V., Margreiter, R. and Kunz, W. S. (2008). Analysis of mitochondrial function *in situ* in permeabilized muscle fibers, tissues and cells. *Nat. Protoc.* **3**, 965-976. doi:10.1038/nprot.2008.61

Lapuente-Brun, E., Moreno-Loshuertos, R., Acín-Pérez, R., Latorre-Pellicer, A., Colás, C., Balsa, E., Perales-Clemente, E., Quirós, P. M., Calvo, E., Rodríguez-Hernández, M. A. et al. (2013). Supercomplex assembly determines electron flux in the mitochondrial electron transport chain. *Science* **340**, 1567-1570. doi:10.1126/science.1230381

Larsen, S., Nielsen, J., Hansen, C. N., Nielsen, L. B., Wibrand, F., Stride, N., Schroder, H. D., Boushel, R., Helge, J. W., Dela, F. et al. (2012). Biomarkers of mitochondrial content in skeletal muscle of healthy young human subjects. *J. Physiol.* **590**, 3349-3360. doi:10.1113/jphysiol.2012.230185

Latorre-Pellicer, A., Moreno-Loshuertos, R., Lechuga-Vieco, A. V., Sánchez-Cabo, F., Torroja, C., Acín-Pérez, R., Calvo, E., Aix, E., González-Guerra, A., Logan, A. et al. (2016). Mitochondrial and nuclear DNA matching shapes metabolism and healthy ageing. *Nature* **535**, 561-565. doi:10.1038/nature18618

Letts, J. A., Fiedorczuk, K. and Sazanov, L. A. (2016). The architecture of respiratory supercomplexes. *Nature* **537**, 644-648. doi:10.1038/nature19774

Lopez-Fabuel, I., Le Douce, J., Logan, A., James, A. M., Bonvento, G., Murphy, M. P., Almeida, A. and Bolaños, J. P. (2016). Complex I assembly into supercomplexes determines differential mitochondrial ROS production in neurons and astrocytes. *Proc. Natl. Acad. Sci. USA* **113**, 13063-13068. doi:10.1073/pnas.1613701113

Maranzana, E., Barbero, G., Falasca, A. I., Lenaz, G. and Genova, M. L. (2013). Mitochondrial respiratory supercomplex association limits production of reactive oxygen species from complex I. *Antioxid. Redox Signal.* **19**, 1469-1480. doi:10.1089/ars.2012.4845

Milenkovic, D., Blaza, J. N., Larsson, N.-G. and Hirst, J. (2017). The enigma of the respiratory chain supercomplex. *Cell Metab.* **25**, 765-776. doi:10.1016/j.cmet.2017.03.009

Nicholls, D. G. (1974). The influence of respiration and ATP hydrolysis on the proton-electrochemical gradient across the inner membrane of rat-liver mitochondria as determined by ion distribution. *Eur. J. Biochem.* **50**, 305-315. doi:10.1111/j.1432-1033.1974.tb03899.x

Pamenter, M. E., Shin, D. S.-H. and Buck, L. T. (2008). AMPA receptors undergo channel arrest in the anoxic turtle cortex. *Am. J. Physiol. Integr. Comp. Physiol.* **294**, R606-R613. doi:10.1152/ajpregu.00433.2007

Pamenter, M. E., Gomez, C. R., Richards, J. G. and Milsom, W. K. (2016). Mitochondrial responses to prolonged anoxia in brain of red-eared slider turtles. *Biol. Lett.* **12**, 20150797. doi:10.1098/rsbl.2015.0797

Papandreou, I., Cairns, R. A., Fontana, L., Lim, A. L. and Denko, N. C. (2006). HIF-1 mediates adaptation to hypoxia by actively downregulating mitochondrial oxygen consumption. *Cell Metab.* **3**, 187-197. doi:10.1016/j.cmet.2006.01.012

Pullman, M. E., Penefsky, H. S., Datta, A. and Racker, E. (1960). Partial resolution of the enzymes catalyzing oxidative phosphorylation I. Purification and properties of soluble, dinitropenol-stimulated adenosine triphosphatase. *J. Biol. Chem.* **235**, 3322-3329.

Schwerzmann, K., Hoppeler, H., Kayar, S. R. and Weibel, E. R. (1989). Oxidative capacity of muscle and mitochondria: correlation of physiological, biochemical, and morphometric characteristics. *Proc. Natl. Acad. Sci. USA* **86**, 1583-1587. doi:10.1073/pnas.86.5.1583

Scott, I. D. and Nicholls, D. G. (1980). Energy transduction in intact synaptosomes. Influence of plasma-membrane depolarization on the respiration and membrane potential of internal mitochondria determined in situ. *Biochem. J.* **186**, 21-33. doi:10.1042/bj1860021

Semenza, G. L. L. (2007). Oxygen-dependent regulation of mitochondrial respiration by hypoxia-inducible factor 1. *Biochem. J.* **405**, 1-9. doi:10.1042/BJ20070389

Semenza, G. L. (2013). HIF-1 mediates metabolic responses to intratumoral hypoxia and oncogenic mutations. *J. Clin. Invest.* **123**, 3664-3671. doi:10.1172/JCI67230

Spinazzi, M., Casarin, A., Pertegato, V., Salviati, L. and Angelini, C. (2012). Assessment of mitochondrial respiratory chain enzymatic activities on tissues and cultured cells. *Nat. Protoc.* **7**, 1235-1246. doi:10.1038/nprot.2012.058

Srere, P. A. (1969). Citrate synthase. *Methods Enzymol.* **13**, 3-11. doi:10.1016/0076-6879(69)13005-0

St-Pierre, J. and Boutilier, R. G. (2001). Aerobic capacity of frog skeletal muscle during hibernation. *Physiol. Biochem. Zool.* **74**, 390-397. doi:10.1086/320428

St-Pierre, J., Charest, P. M. and Guderley, H. (1998). Relative contribution of quantitative and qualitative changes in mitochondria to metabolic compensation during seasonal acclimatisation of rainbow trout *Oncorhynchus mykiss*. *J. Exp. Biol.* **201, 2961-2970**.

St-Pierre, J., Brand, M. D. and Boutilier, R. G. (2000a). Mitochondria as ATP consumers: cellular treason in anoxia. *Proc. Natl. Acad. Sci. USA* **97**, 8670-8674. doi:10.1073/pnas.140093597

St-Pierre, J., Tattersall, G. J. and Boutilier, R. G. (2000b). Metabolic depression and enhanced O_2 affinity of mitochondria in hypoxic hypometabolism. *Am. J. Physiol. Integr. Comp. Physiol.* **279**, R1205-R1214. doi:10.1152/ajpregu.2000.279.4.R1205

Stecyk, J. A. W., Bock, C., Overgaard, J., Wang, T., Farrell, A. P. and Pörtner, H.-O. (2009). Correlation of cardiac performance with cellular energetic components in the oxygen-deprived turtle heart. *Am. J. Physiol. Regul. Integr. Comp. Physiol.* **297**, R756-R768. doi:10.1152/ajpregu.00102.2009

Trounce, I. A., Kim, Y. L., Jun, A. S. and Wallace, D. C. (1996). Assessment of mitochondrial oxidative phosphorylation in patient muscle biopsies, lymphoblasts, and transmitochondrial cell lines. *Methods Enzymol.* **264**, 484-509. doi:10.1016/S0076-6879(96)64044-0

Ultsch, G. R. (1985). The viability of nearctic freshwater turtles submerged in anoxia and normoxia at 3 and 10°C. *Comp. Biochem. Physiol. A Physiol.* **81**, 607-611. doi:10.1016/0300-9629(85)91035-7

Ultsch, G. R. (2006). The ecology of overwintering among turtles: where turtles overwinter and its consequences. *Biol. Rev. Camb. Philos. Soc.* **81**, 339-367. doi:10.1017/S1464793106007032

Van Coster, R., Smet, J., George, E., De Meirleir, L., Seneca, S., Van Hove, J., Sebire, G., Verhelst, H., De Bleecker, J., Van Vlem, B. et al. (2001). Blue native polyacrylamide gel electrophoresis: a powerful tool in diagnosis of oxidative phosphorylation defects. *Pediatr. Res.* **50**, 658-665. doi:10.1203/00006450-200111000-00020

Warren, D. E., Reese, S. A. and Jackson, D. C. (2006). Tissue glycogen and extracellular buffering limit the survival of red-eared slider turtles during anoxic submergence at 3°C. *Physiol. Biochem. Zool. PBZ* **79**, 736-744. doi:10.1086/504617

Wasser, J. S., Meinertz, E. A., Chang, S. Y., Lawler, R. G. and Jackson, D. C. (1992). Metabolic and cardiodynamic responses of isolated turtle hearts to ischemia and reperfusion. *Am. J. Physiol.* **262**, 437-443. doi:10.1152/ajpregu.1992.262.3.R437

Weibel, E. R. (1979). *Stereological Methods: Vol.: 1. Practical Methods for Biological Morphometry*. London: Academic Press.

Willmore, W. G. and Storey, K. B. (1997a). Antioxidant systems and anoxia tolerance in a freshwater turtle *Trachemys scripta elegans*. *Mol. Cell. Biochem.* **170**, 177-185. doi:10.1023/A:1006817806010

Willmore, W. G. and Storey, K. B. (1997b). Glutathione systems and anoxia tolerance in turtles. *Am. J. Physiol.* **273**, 219-225.

Yellon, D. M. and Hausenloy, D. J. (2007). Myocardial reperfusion injury. *New Engl. J. Med. Rev.* **357**, 1121-1135. doi:10.1056/NEJMra071667

Zhang, H., Bosch-Marce, M., Shimoda, L. A., Tan, Y. S., Baek, J. H., Wesley, J. B., Gonzalez, F. J. and Semenza, G. L. (2008). Mitochondrial autophagy is an HIF-1-dependent adaptive metabolic response to hypoxia. *J. Biol. Chem.* **283**, 10892-10903. doi:10.1074/jbc.M800102200